Highly Accelerated Whole Brain Imaging Using Aligned-Blipped-Controlled-aliasing Multiband EPI

Junqian Xu[1], Steen Moeller[1], John Strupp[1], Edward J. Auerbach[1], Liyong Chen[2,3], David A. Feinberg[2,3], Kamil Ugurbil[1], Essa Yacoub[1]

[1]Center for Magnetic Resonance Research, University of Minnesota, Minneapolis, MN, United States; [2]Helen Wills Neuroscience Institute, University of California, Berkeley, CA, United States; [3]Advanced MRI Technologies, Sebastopol, CA, United States

Introduction High-resolution whole brain imaging increases volume acquisition time (TR), limiting the number of data points and temporal efficiency in EPI-based scans for fMRI, diffusion and perfusion imaging. We recently developed and applied simultaneous slice imaging [1] in fMRI for "slice accelerated" multiband (MB) EPI to achieve significant reductions in whole brain acquisition times without substantial degradation in image quality or SNR [2]. In this technique, several slices are simultaneously excited using a single multi-banded RF pulse and subsequently un-aliased using parallel imaging principles. Setsompop et al. [3] recently introduced modulation of the slice gradient blip-based controlled aliasing technique [4] for EPI, modified from Nunes et al. [5], which balanced the gradient blips with periodic rewinder to eliminate voxel tilt blurring. By shifting apart simultaneously acquired slices on the phase encode axis with controlled aliasing, g-factors can be significantly reduced, permitting higher slice accelerations. To achieve even higher slices accelerations and to reduce problematic phase errors in EPI acquisitions, we propose here a *k*-space center (k_0) alignment strategy as opposed to a pure balancing blip approach [3].

Methods ABC-MB EPI (Aligned-Blipped-Controlled-aliasing MultiBand EPI): A G_z pre-blip was used (Fig. 1, middle row, dotted) to align the *k*-space center (k_0) line to be fully refocused (Fig. 1, bottom row) instead of a strictly balanced approach [3], where a non-zero gradient moment can remain at the echo time of the *k*-space center (k_0) line (similar to Fig. 1, top row).

Gradient echo ABC-MB EPI images were acquired using a 32-channel head coil on a 3 T scanner (Connectom Skyra with SC72 gradients, Siemens). Oblique transaxial images were collected (FOV 192×192 mm, matrix 96×96, slice thickness 2 mm, TR/TE 4800/30 ms, flip angle 55°, controlled aliasing PE_{Shift} = ¼ FOV, sinc excitation pulse width 12.8 ms) with 64 slices. For comparison, a long TR and matched flip angles were used for all acquisitions (up to MB12, Fig. 2). In addition, controlled aliasing using balanced-blips [3] were collected (MB = 4, 6, and 8, Fig. 3) for comparison with ABC approach. To evaluate the robustness of high slice acceleration factors and subsequent high temporal resolutions, we acquired time series (MB=1, 4, 6, and 8, resolution 2 mm isotropic, TR/TE = 67/30 ms, flip angle 20°, ~5 minutes) for spectral comparison and analysis. MB1 was a single slice acquired at minimum TR. MB4, 6, and 8 used the same minimum TR (67 ms) but acquired multiple slices simultaneously. One of these slices was always matched to the single slice acquired in MB1. For all MB>1 acquisitions, a PE_{Shift} = ¼ FOV was used.

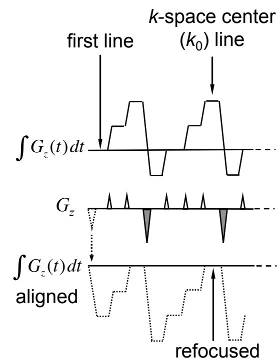

Figure 1. Aligned-Blipped-Controlled-aliasing strategy (e.g., PE_{Shift} = ¼ FOV)

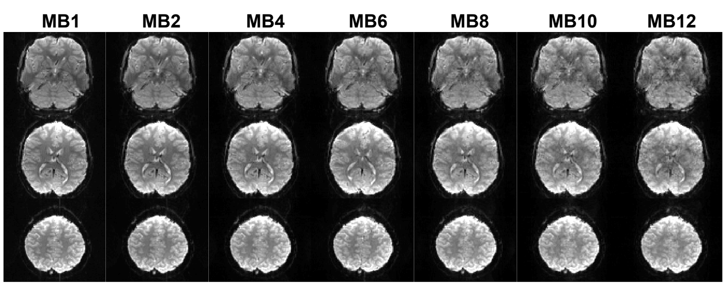

Figure 2. Slice acceleration up to a factor of 12 demonstrates negligible image degradation up to MB4 and good image quality up to ~MB8 to 10.

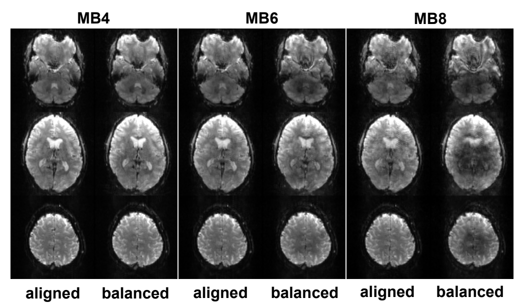

Figure 3. ABC-MB (aligned) demonstrates less image degradation than balanced-blip MB for high MB factors.

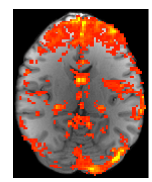

Figure 4. Spatial coherence map of MB8 at cardiac frequency (0.87 Hz) overlaid on anatomical image.

Spectral Analysis: Each acquired slice in the single-shot datasets was first 2D motion-corrected. Spectral consistency between the datasets acquired with increasing MB factors were assessed by verifying the correspondence of noise content from the monitored physiologic data using an average of the power spectral density (PSD) estimates of individual time-series calculated using multi-taper methods [6]. A space-frequency SVD for energy partitioning for the formation of an aggregate spectrum was used. In this method, each time series in the dataset is first projected down to a frequency interval prior to the performing SVD. The coherence is then assessed for that frequency interval as the percentage of the energy that is captured by the dominant singular value. The process is repeated at each frequency across the band of spectral interest up to the Nyquist limit [7].

Results and Discussion ABC-MB EPI permitted much higher slice acceleration than was possible using a strictly balanced blip approach, while also preserving minimal phase accrual during the readout train, which eliminates voxel tilting dependent blurring along the slice direction [3]. The g-factors and residual aliasing effects due to the high acceleration factors were quantified using unique methods (Moeller et al. submitted) [8]. These were shown to be significantly reduced with the ABC-MB approach employed here - with the high MB levels being comparable to previously published results at lower MB factors, demonstrating robust artifact free detection of typical resting state networks [9]. Further, the results show that spectral characteristics are preserved across the different slice accelerations (Fig. 4), while also permitting extended volume coverage with the same fast TR. This technique could be used for alias-free sampling of cardiac fluctuations in EPI based fMRI, preventing spectral folding and subsequent contamination of neuronal effects or for highly efficient prospective gating to reduce motion effects in diffusion imaging. Further, as previously demonstrated [9], fMRI statistical power can be improved due to the increase in temporal efficiency, permitting improved delineation of functional networks and/or reduced scan times.

Reference [1] Larkman, et al. *J. Mag. Res. Img.* 13:313-317, 2001 [2] Moeller, et al. *Magn. Reson. Med.* 63:1144–53, 2010 [3] Setsompop, et al. *Magn. Reson. Med*. 2011 in press [4] Breuer, et al. *Magn. Reson. Med*. 53:684–91, 2005 [5] Nunes, et al. ISMRM 2006 [6] Mitra et al., *Magn. Reson. Med.* 378:511-518, 1997 [7] Mitra et al., *Biophys. J.* 76:691-708, 1999 [8] Moeller, et al. ISMRM 2012 [9] Feinberg, et al. PLoS ONE, 5(12):e15710, 2010

Acknowledgements Funded by the NIH Human Connectome Project (U54MH091657), as well as NIH grants, R44 NS073417, P41 RR008079 and P30 NS057091.